Review of Palaeobotany and Palynology 312 (2023) 104860

Contents lists available at ScienceDirect

Review of Palaeobotany and Palynology

journal homepage: www.elsevier.com/locate/revpalbo

The 3D Pollen Project: An open repository of three-dimensional data for outreach, education and research

Oliver J. Wilson [a,b,*]

[a] School of Archaeology, Geography and Environmental Science, University of Reading, Wager Building, Pepper Lane, Whiteknights, Reading RG6 6EJ, UK
[b] Department of Environment and Geography, University of York, Wentworth Way, Heslington, York YO10 5NG, UK

ARTICLE INFO

Article history:
Received 5 January 2023
Received in revised form 7 February 2023
Accepted 8 February 2023
Available online 14 February 2023

Keywords:
3D pollen
3D printing
Outreach and engagement
Confocal microscopy
Open-access database

ABSTRACT

Pollen is vitally important in the natural world, the scientific research which studies it, and society at large. Pollen is beautiful and immensely resilient, records millions of years of evolutionary, ecological and climatic change, underpins globally critical ecosystem functions and services, helps solve crimes, could revolutionise medicine – and, as one of humanity's most significant allergens, irritates hundreds of millions of people around the world. However, engaging non-specialists with pollen-related research can be challenging, because pollen's microscopic nature means all interactions with it must be visual, predominantly through static two-dimensional images (which obscure the grains' full 3D nature and beauty), complex stratigraphic diagrams (which can be impenetrable to non-specialists), or specialist microscopy (which adds complexity and expense). A recent development has been to use accurate and larger-than-life 3D-printed models, allowing audiences to interact with pollen and related research in new, tactile ways.

This paper introduces the 3D Pollen Project, an open-access repository of 3D pollen scans and surface files. Confocal laser scanning microscopy was used to produce accurate series of tightly-focused cross-section images through pollen grains, which were reconstructed to produce 3D-printable surface files; both specific methods and underpinning general principles are outlined to enable others to emulate the work. Matching the refractive indices of sample mountant and objective lens immersion medium is shown to be particularly important for producing high-quality scans. The 35 species included in the 3D Pollen Project to date cover a broad (if Euro-centric) geographic distribution and a comprehensive suite of pollen's morphological features. These models, made available online for free download, have been used in a very wide range of contexts around the world, in outreach, education and research. Finally, future steps for the 3D Pollen Project are discussed: growing its coverage into a truly globally representative sample of global pollen diversity; enhancing the quality of its data; and developing the ways in which its resources are used.

1. Introduction

Pollen is an immensely important substance in the natural world, in the scientific research which studies it, and in wider society. (In this paper, 'pollen' refers collectively to true pollen and other plant spores.) The development of protective shells made from sporopollenin – 'the diamond of the plant world' (Kesseler and Harley, 2009, p. 44), 'one of the most extraordinarily resistant materials known in the organic world' (Faegri and Iversen, 1964, p. 15) – likely played a key role in facilitating plants' colonisation of Earth's land surface (Guzmán-Delgado and Zwieniecki, 2019; Li et al., 2019; Wallace et al., 2011). Grains preserved for hundreds of millions of years record plants' subsequent evolutionary trajectories (Morris et al., 2018; Rubinstein et al., 2010; Wellman, 2010), and modern studies of pollen's architecture help scientists understand the taxa that have arisen (e.g. Banks and Rudall, 2016). Fossil pollen grains record many millennia of climate and vegetation change (e.g. Mottl et al., 2021; Rull et al., 2016; Williams et al., 2004), from the cataclysmic origins of modern neotropical rainforests (Carvalho et al., 2021) to the long-term legacies of sustainable land use by Indigenous communities (Kelly et al., 2018; Maezumi et al., 2018), and their study has been described as 'the single most important branch of terrestrial palaeoecology for the late Pleistocene and Holocene' (Roberts, 2014, p. 33). Since pollen first evolved, its flow between plants and across landscapes has been critical for supporting species, populations and ecosystems – and, in the modern day, it also has immense economic value for humans, with global pollination services worth hundreds of billions of dollars a year for crops alone (Porto et al., 2020). Pollen's societal importance goes beyond its ecosystem functions, too: pollen grains are one of the world's most significant

* Corresponding author.
E-mail address: oliver.wilson@york.ac.uk (O.J. Wilson).

https://doi.org/10.1016/j.revpalbo.2023.104860

allergens (affecting hundreds of millions of people, perhaps 30% of the global population; D'Amato et al., 2007; Pawankar et al., 2013), help verify honey sources (Holt and Bebbington, 2014), signal the presence of oil reservoirs (Rodrguez-Forero et al., 2012), have potential as targeted delivery vehicles for medicines and vaccines (Atwe et al., 2014; Harris et al., 2016; Mackenzie et al., 2015; Uddin and Gill, 2018), and can even play a role in solving crimes (Mildenhall, 2008).

But despite its multifaceted importance in so much of nature, science and life, pollen can be a challenging subject with which to engage non-specialist audiences. Pollen grains are microscopic so they cannot be held, and while they can be seen, this generally requires specialist equipment and the cost, expertise and inconveniences this often entails. Furthermore, while microscopes and the images they produce can convey to lay observers something of pollen's appearance, it is inherently challenging to interpret pollen's three-dimensional reality from these two-dimensional images. This difficulty also afflicts the teaching of pollen identification skills (which underpin many of palynology's applications) – some instructors hand-make rough physical models to help convey pollen's principal features.

Generating biologically accurate, larger-than-life 3D models of pollen grains can greatly assist with these challenges (Ball et al., 2017; Holt and Savoian, 2017; Perry et al., 2017; Stevenson and Kaikkonen, 2019). 3D-printed models make pollen both tactile and readily visible, significantly lowering the bar to engagement for non-specialists. Such models can also help demonstrate key concepts in pollen identification, from the appearance of diagnostic features to the relationship between light micrograph cross-sections and the whole pollen grain. There are two main approaches to creating such 3D pollen models.

The first approach is to sculpt pollen grains' likenesses from micrographs, which can be done physically or (more commonly) in computer-aided design (CAD) software. This approach needs relatively little specialist equipment but does require the sculptor to have some palynological literacy as well as the technical skill to produce an accurate likeness. There are few technological limitations on how the model can be designed, and imperfections in specific pollen samples can be overlooked in favour of an idealised, more universal depiction, but accurately capturing realistic elements of pollen form and structure (particularly internal architecture and individual variations between grains) may be very difficult. Pollen models have been developed using this process as part of the FRAGSUS Project (Fragility and sustainability in small island environments: adaptation, cultural change and collapse in prehistory) (French et al., 2020; models available from https://sketchfab.com/1manscan, accessed 15/06/2021), for the Lake Biwa Museum, Japan (models can be viewed at https://sketchfab.com/rcgear_japan, accessed 22/12/2022), and at the BEAST (Biodiversity and Environments Across Space and Time) Lab at the University of Maine, USA (models not available online).

The second approach to producing 3D pollen data is to directly scan pollen samples, generally with confocal microscopy (Holt and Savoian, 2017; Perry et al., 2017; Stevenson and Kaikkonen, 2019; Vitha et al., 2010) or SEM-microphotogrammetry (Ball et al., 2017). Evidently, these equipment requirements represent a much higher bar to accessibility than the sculpture method, but the approach has several significant benefits. After initial technical training on the imaging platforms, the scanning process can be quick, with relatively high sample throughput (Romero et al., 2020b). Although technical limitations (such as a microscope's resolving power) may compromise some aspects of a resulting model's realism (Holt and Savoian, 2017), directly scanning pollen samples means that typical, unusual and/or damaged examples can all be accurately and easily represented. Critically, valuable microscopy data is also generated in the scanning process. This means that photomicrographs can be taken alongside 3D scans, allowing different representations of the same samples to be cross-referenced (Collings, 2015; Romero et al., 2020b). Fine-scale sculptural details or internal structures can also be captured to show a grain's identifying features in images or models. The scan data can even be put to uses other than purely 3D reconstruction, such as the development of automated pollen identification (Holt and Bebbington, 2014; Romero et al., 2020a).

Several groups have produced 3D pollen models using confocal microscopy. Holt and Savoian (2017) pioneered the approach at Massey University, combining imaging methods from Vitha et al. (2010) with 3D printing to produce physical models of several New Zealand pollen taxa (the models are not available online). Using similar techniques, Cardiff University's Bioimaging Hub has built up a significant collection of scans from disparate taxa, with 3D surface models of 68 taxa available online (Perry et al., 2017; https://3dprint.nih.gov/users/cubioimaginghub/); the Australian 3D Pollen Project (Australian National University) has also scanned and made available surface files of 13 Australian pollen types (Stevenson and Kaikkonen, 2019; http://www.doi.org/10.25911/5d0ac8204ae57). In neither of these cases, however, are the original microscopy data available. Conversely, the Punyasena Palaeoecology Lab at the University of Illinois Urbana-Champaign has made available dozens of image stacks from several fossil and extant pollen taxa in the Amherstieae tribe of the Fabaceae (subfamily Detarioideae), but these have not been processed into surface files (Romero et al., 2020a; https://doi.org/10.13012/B2IDB-9133967_V1). Therefore, although several independent teams have successfully demonstrated that confocal microscope scans of pollen grains can be made and converted into accurate 3D-printable models, these datasets are generally limited in taxonomic or geographic scope, partially complete (containing scans or surface files, but not both), and/or inaccessible for most interested parties.

This paper introduces the 3D Pollen Project (https://3dpollenproject.wixsite.com/main/), which aims to complement and extend these initiatives. Using confocal microscopy, the project has produced accurate scans and 3D-printable surface models of pollen from a geographically and taxonomically broad range of taxa, and makes the resulting scan and surface data freely available online. At time of writing, the 3D Pollen Project has the world's largest open-source collection of linked scans and surface models, initially comprising 39 samples from 35 taxa. The following sections set out the general principles behind the project's methods and the specifics of how they have been applied in its work so far; assesses the project's outputs to date and the ways they have been used in outreach, education and research; and describes its future directions and pathways to creating a high-quality, globally representative sample of the world's pollen diversity.

2. Methods

There are four main steps in the production of 3D-printed pollen models: obtaining and processing pollen material, image acquisition with a confocal laser scanning microscope (CLSM), image processing, and 3D printing (summarised in Fig. 1). The first part of the methods section (Section 2.1) provides a general overview of these approaches, alongside key principles and considerations for their application. This section can be used as a guide for local adaptation of the specific methods used in the 3D Pollen Project so far (Section 2.2). It can also act as a scaffold for evaluating whether and how other, non-pollen, palynomorphs could be scanned in a similar way. Additional guidance on aspects of the preparation, imaging, processing and printing approaches can be found in Vitha et al. (2010), Holt and Savoian (2017), Perry et al. (2017), Stevenson and Kaikkonen (2019), and Romero et al. (2020b).

2.1. Overview and general principles

CLSMs use precise wavelengths of light to excite samples, and a pinhole which blocks out-of-focus emissions from the samples from being detected. Narrowing the pinhole improves resolution but reduces signal strength, with the optimal compromise found at a pinhole diameter of 1 Airy Unit. The resulting images are tightly focused cross-sections of the

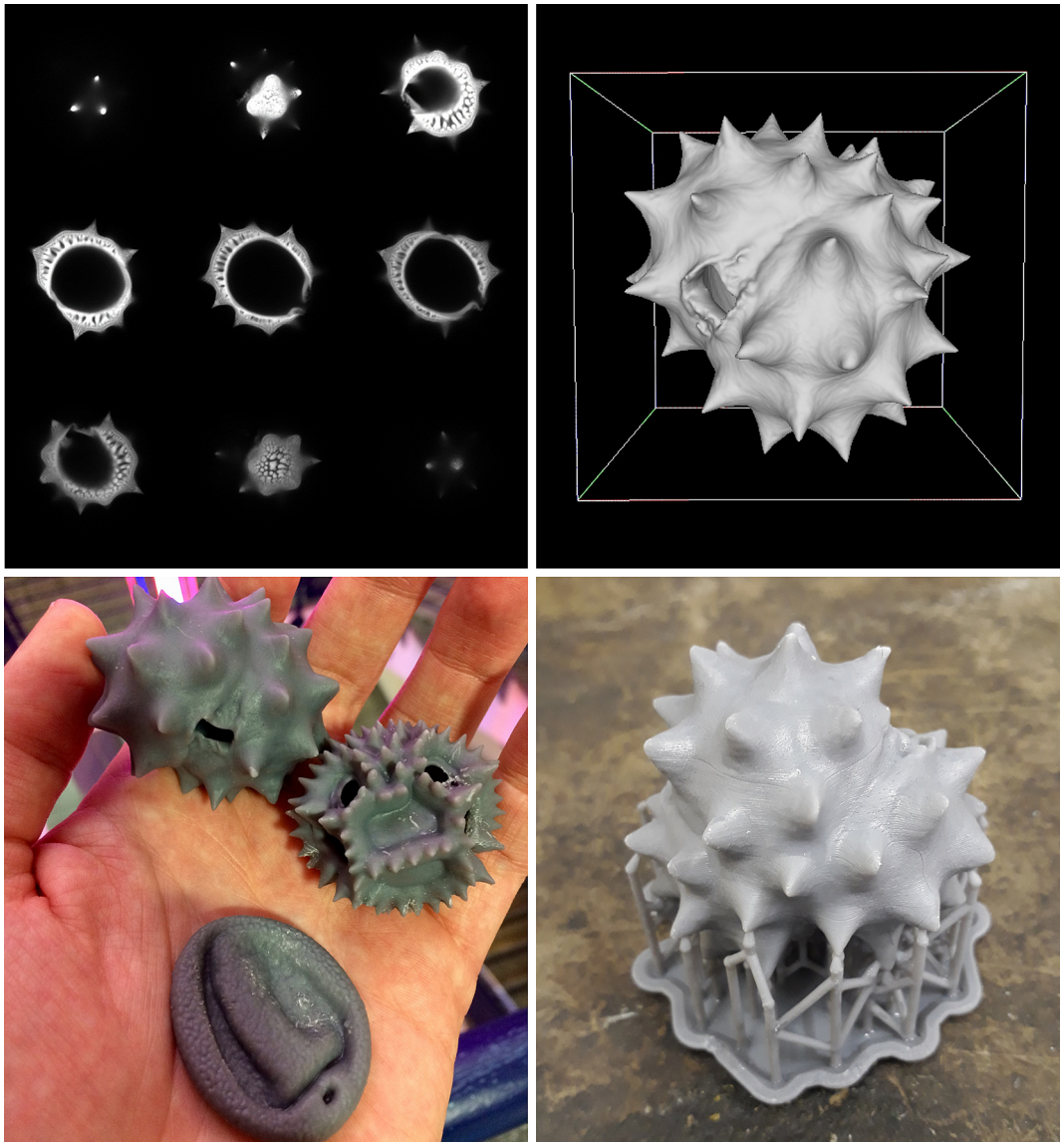

Fig. 1. An illustrative overview of the main steps in producing 3D pollen models. Clockwise from top left: confocal microscopy scans of a *Leucanthemum vulgare* (Asteraceae) pollen grain, conversion of an 89-image stack of microscopy data into a virtual surface model, a model 3D-printed using a resin printer (before removal of support structures), and cleaned pollen models (from top to bottom: *L. vulgare*, *Scorzoneroides autumnalis*, and *Dactylis glomerata*) ready for use.

fluorescent material at a given depth in the sample. By producing a series of these images taken at tightly-spaced intervals along the z axis – a 'z stack' – a three-dimensional representation of a pollen grain can be built up, and this can be converted into a model of the grain's surface.

Confocal microscopy requires that samples fluoresce when excited by laser light, which is often achieved by the addition of fluorescent dyes. Since pollen grains autofluoresce under a wide spectrum of laser wavelengths, however, such dyes are not necessary, though they can improve signal-to-noise ratios in scan images (Sivaguru et al., 2018). It is possible to scan unprocessed pollen grains (Perry et al., 2017), but pollen's cell contents absorb both emitted and excited light and can drastically reduce the strength of the signal detected from lower parts of the grain – which in any case are attenuated by travelling through the grain's upper exine (Vitha et al., 2010). For this reason, it is preferable to acetolyse pollen grains, removing their cell contents to leave a cleaned, hollow exine, before scanning with a CLSM.

Reference slides of modern pollen and research slides of (sub-)fossil pollen are commonly acetolysed prior to mounting, but CLSM scans of this material are often compromised by the choice of mountant. In palaeoecology, pollen samples are generally mounted in silicone oil or glycerine jelly, which allow grains to be rotated for easier identification. This mobility can present problems for confocal scanning when grains shift during imaging (Romero et al., 2020b), but a more significant challenge is refractive index (RI) mismatch (Diel et al., 2020; Vitha et al., 2010). The most common high-magnification, high-resolution microscope objective lenses use immersion oil, which has an RI of ca. 1.52; this is mismatched with both silicone oil (RI 1.41) and glycerine jelly (RI 1.46–1.47). Such RI mismatches disrupt the light path between laser, sample, objective lens and detector, resulting in increasing loss of signal with sample depth, diminished resolution along the z axis, and spherical aberration. These problems are illustrated in the present manuscript's fig. 5, Staudt et al. (2007, fig. 6), and Diel et al. (2020). It is preferable, therefore, to mount acetolysed pollen in a medium whose refractive index very closely matches the immersion medium of the CLSM's objective lens

Correctly processed and mounted pollen slides can then be scanned with a confocal microscope. It is important to note that the resolution of the scans is always poorer along the z (depth) axis than in x and y. This

can be illustrated by reference to the Houston criterion for defining resolution (full width at half maximum, FWHM; eq. 1):

$$FWHM_{xy} = \frac{0.51 \times \lambda}{NA}$$

$$FWHM_{z} = \frac{1.77 \times RI \times \lambda}{NA^2}$$

λ = excitation wavelength,
NA = numerical aperture of the objective lens,
RI = refractive index of the immersion medium.

For a microscope using a 488 nm laser, 1.4 NA objective, and a sample in a medium with an RI of 1.518, the FWHM resolution would be 178 nm in xy and 669 nm in z. Using lenses with higher numerical apertures improves scan resolution, as does closing the pinhole, though the greatest increase in resolution is available through super-resolution technologies such as AiryScan, which uses an array of detectors with tightly closed pinholes to increase resolution 1.7 times in all axes, as well as providing a 'virtual NA boost' (Romero et al., 2020b; Sivaguru et al., 2018; Weisshart, 2014).

When a z stack of scans has been produced (the number of slices depends on the size of the sample and the spacing between images), it can be converted into a surface file in image processing software. The simplest way is to apply a single threshold value to the stack, transforming the continuous variable of signal strength to a binary of solid or void. Variations in signal strength with sample depth can be pronounced in pollen scans, so a single threshold value may not always be suitable – one that accurately discriminates exine from empty space at layers with stronger signal may miss out surfaces at lower slices with weaker signal, and vice versa. This can be resolved in several ways: in image capture, laser intensity can be programmed to increase with sample depth so that contrast remains constant through the stack; contrast can also be increased with depth in post-processing; and more advanced approaches to thresholding – such as trainable image segmentation algorithms – can be used. The surface files derived from thresholded image stacks can be saved in an appropriate format (such as .stl), then viewed online, virtually manipulated, and/or 3D-printed.

There are various 3D printing techniques, most of them forms of additive manufacturing – the sequential build-up of layers of material (generally plastics) to form a three-dimensional object. Two of the most widely available 3D printing technologies are fused filament fabrication/fused deposition modelling (FFF/FDM) and vat polymerisation (resin printing). FFF/FDM printers have mobile nozzles which melt and extrude filament in patterns which cool and re-solidify on a build plate to form individual layers of the model. Resin printers use vats of photosensitive resin, which solidifies when it is illuminated by a light source projecting the shape of the desired layer onto a build plate. Each technology has strengths and weaknesses for producing 3D pollen models. Resin printers are excellent at producing complex, high-detail models, especially at small sizes; they can also effectively use translucent/transparent materials. FFF/FDM printers are generally less capable with combinations of small size and high complexity, being instead more suited to producing larger prints, although they are generally cheaper and compatible with a wider range of materials than resin. Both FFF/FDM and resin printers add supporting structures to complex shapes (such as overhangs) which need to be removed after printing is finished; resin printers must also add small holes to sealed hollow chambers to allow uncured resin to escape. It is important, too, to note that the cost of 3D printing scales with the amount of material used, and therefore with model size and complexity.

2.2. 3D Pollen Project methods

At time of publication, the majority of samples used in the 3D Pollen Project were processed from herbarium specimens, with others remounted from pre-existing reference material (Table 1). Pollen-bearing structures were removed from herbarium specimens (see Jarzen and Jarzen, 2006), then washed in hot 10% potassium hydroxide solution, sieved and acetolysed. After acetolysis, samples were transferred to distilled water, which was gradually replaced by increasing concentrations of 2,2′-thiodiethanol (TDE) (Holt and Savoian, 2017; Vitha et al., 2010). TDE is a water-soluble mounting medium whose refractive index varies with concentration (from 1.33 at 0% to 1.52 at 100%), so it can be tuned to match the immersion medium of an objective lens (Staudt et al., 2007). Following the suggested concentration increments of Staudt et al. (2007), TDE was added stepwise to the suspended pollen samples, allowed to rest for 5–10 min, then centrifuged with the supernatant decanted. After several immersions in a solution of approximately 97% TDE by volume, the samples were mounted on slides and sealed with either paraffin wax or clear nail varnish.

Pollen samples were scanned with a Zeiss LSM710 confocal microscope at the University of Hull, UK, using a 63×/1.4 NA oil immersion objective lens. For most samples the pinhole diameter was set to 1 AU, though in cases where low z-axis resolution was more problematic than signal loss this was reduced to 0.66 AU. Samples were scanned with relatively high laser intensity and relatively low detector gain. Increasing laser power provides more signal but bleaches the pollen; increasing gain across the detector boosts both signal and noise but allows for gentler laser illumination. Since laser-bleached pollen grains still scan well and do not seem to suffer other visible damage, and since the samples scanned were not otherwise in use as reference material (where bleaching may be more problematic), signal improvements from increased laser power were deemed preferable to those from increased detector gain. Z stacks were acquired through entire pollen grains (including some additional space above and below the grain), with sections spaced using the optimal z interval calculated according to the Nyquist criterion.

In stacks where loss of signal with depth was pronounced, either laser intensity was set to increase through the sample, or contrast in the lower half of the z stack was increased post-acquisition using the 'Processing – Adjust – Interpolate brightness and contrast' tool in Zeiss's Zen software. The resulting .lsm files were saved and exported for 3D rendering in open-source software.

Image stacks were converted to surface files using Fiji/ImageJ (Schindelin et al., 2012). To reduce 'stepping' effects along the z axis, the stacks were resliced and interpolated to have cubic voxels (i.e., equal-sized axes in x, y and z), then converted to 8-bit images for compatibility with Fiji/ImageJ's 3D viewer plugin (Schmid et al., 2010). Threshold values were chosen by examining signal strength (pixel values) in exine features on the z stack's lower slices (i.e., those with lower signal intensity), and selecting a value which effectively discriminated solid and void at these layers. This threshold value was then used as input when opening the resliced 8-bit image stack in Fiji/ImageJ's 3D viewer plugin, converting the images to a surface file. If this approach to thresholding failed, Fiji/ImageJ's Trainable Weka Segmentation 3D plugin (Arganda-Carreras et al., 2017) was used (the software includes several other binarizing algorithms) and the resulting binary image imported to the 3D viewer. When examination of the 3D surface showed that a satisfactory threshold had been chosen, the surface mesh was exported as an .stl file.

To improve the suitability of the exported .stl surface files for 3D printing, they were further processed in MeshLab (Cignoni et al., 2008). MeshLab interpreted surface meshes processed in Fiji/ImageJ from CLSM scans as 'inside out', which was addressed by inverting the orientation of the meshes' surfaces. CLSM-derived surface files are generally extremely detailed, with hundreds of thousands of vertices and faces. Reducing their complexity makes file sizes smaller and 3D printing easier – and can be done without loss of detail in the final physical model, if the original mesh is more detailed than the printer can represent. Combinations of quadric edge collapse decimation and HC Laplacian smoothing were used on the meshes, with the contributions

Table 1
The 35 taxa included in the 3D Pollen Project to date. Sample codes identify the institution, collection, and specimen scanned. CHIC-EchProj: the Chicago Botanic Garden Echinacea Project; EXR-EXPR: the University of Exeter tropical pollen reference collection; HLU-CCC: the Crackles Comparative Collection at the University of Hull; MANCH-PolRefCol: the University of Manchester pollen reference collection; RNG-P…: the University of Reading herbarium; RNG-TPRG: the University of Reading tropical pollen reference collection. Where 'incid' occurs at the end of a sample code, it indicates that a pollen grain was found incidentally on a slide from another specimen; these pollen grains were identified by eye to appropriate taxonomic resolution.

Family	Species	Sample code	Source
Anacardiaceae	*Spondias* sp.	EXR-EXPR-86	Pollen reference collection
Araliaceae	*Hedera helix* L.	RNG-P0042298	Herbarium specimen
Arecaceae	*Oenocarpus bacaba* Mart.	EXR-EXPR-95	Pollen reference collection
Asteraceae	*Ambrosia psilostachya* DC.	RNG-P0042299	Herbarium specimen
	Artemisia annua L.	RNG-P0043202	Herbarium specimen
	Centaurea nigra L.	HLU-CCC-4	Herbarium specimen
	Echinacea angustifolia DC.	CHIC-EchProj-1088	Herbarium specimen
	Leucanthemum vulgare Lam.	HLU-CCC-61	Herbarium specimen
	Scorzoneroides autumnalis (L.) Moench	HLU-CCC-174	Herbarium specimen
Betulaceae	*Alnus glutinosa* (L.) Gaertn.	HLU-CCC-444	Herbarium specimen
	Betula pendula Roth	HLU-CCC-595	Herbarium specimen
	Corylus avellana L.	HLU-CCC-413incid	Herbarium specimen
Bignoniaceae	*Handroanthus impetiginosus* (Mart. ex DC.) Mattos	EXR-EXPR-131	Pollen reference collection
Cannabaceae	*Celtis iguanaea* (Jacq.) Sarg.	RNG-TPRG-210	Pollen reference collection
Chenopodiaceae	*Chenopodium album* L.	RNG-P0003852	Herbarium specimen
Cyperaceae	*Carex lasiocarpa* Ehrh.	RNG-P0020162	Herbarium specimen
Ericaceae	*Calluna vulgaris* (L.) Hull	HLU-CCC-695	Herbarium specimen
Fabaceae	*Anadenanthera colubrina* (Vell.) Brenan	RNG-TPRG-199	Pollen reference collection
Fagaceae	*Quercus petraea* (Matt.) Liebl.	HLU-CCC-413	Herbarium specimen
	Quercus robur L.	HLU-CCC-731	Herbarium specimen
Lamiaceae	*Salvia pratensis* L.	RNG-P0042296	Herbarium specimen
Malvaceae	*Tilia cordata* Mill.	RNG-P0042292	Herbarium specimen
Melastomataceae	*Miconia chamissois* Naudin	EXR-EXPR-312	Pollen reference collection
Pinaceae	*Cedrus atlantica* (Endl.) Manetti ex Carrière	MANCH-PolRefCol-MA_AZR_72	Pollen reference collection
	Cedrus deodara (Roxb. ex D.Don.) G.Don.	MANCH-PolRefCol-UK_WB_05_WB110159	Pollen reference collection
	Cedrus libani A.Rich.	MANCH-PolRefCol-UK_MAN_10	Pollen reference collection
	Pinus sp.	HLU-CCC-731incid	Herbarium specimen
Plantaginaceae	*Plantago lanceolata* L.	HLU-CCC-723	Herbarium specimen
Poaceae	*Dactylis glomerata* L.	HLU-CCC-67	Herbarium specimen
	Hordeum murinum L.	RNG-P0042300	Herbarium specimen
	Indet. sp.	HLU-CCC-444incid	Herbarium specimen
Rosaceae	*Filipendula ulmaria* (L.) Maxim.	HLU-CCC-43	Herbarium specimen
Salicaceae	*Salix caprea* L.	RNG-P0042291	Herbarium specimen
Sapindaceae	*Acer campestre* L.	RNG-P0042294	Herbarium specimen
Winteraceae	*Drimys winteri* J.R.Forst. & G.Forst.	RNG-P0042290	Herbarium specimen

of each tool chosen based on a visual examination of their effects on each pollen model. Finally, the smoothed and simplified meshes were rescaled to be 2500× life size when voxel units are interpreted as mm, so that a pollen grain 20 μm in diameter would produce a model 50 mm across without further rescaling.

Original z stacks, converted to .tif file format for wider compatibility but otherwise unprocessed, cross-section animations, and printable .stl surface files are all available for free download from the MorphoSource repository (https://www.morphosource.org/Detail/ProjectDetail/Show/project_id/627) under a Creative Commons CC-BY-NC licence, permitting non-commercial use of the materials with acknowledgement of their source. A range of physical models have been 3D-printed, most of them by the commercial printing service at the UK company 3D Tomorrow (https://3dtomorrow.com). The largest models were produced at 2500× life size (ranging from 44 × 44 × 47 mm for *Filipendula ulmaria* to 98 × 200 × 139 mm for *Pinus* sp.) using an FFF/FDM printer working in polylactic acid (PLA), and the smallest were at 500× life size (20% of the downloaded size, 9 × 9 × 10 mm for *F. ulmaria* and 20 × 40 × 28 mm for *Pinus* sp.) using a resin printer.

2.3. 3D Pollen Project samples

As of late 2022, 39 scans of 35 species have been produced and made available online (https://www.morphosource.org/Detail/ProjectDetail/Show/project_id/627; Table 1). Nine samples were procured from pre-existing pollen reference collections, and the other 26 were processed directly from herbarium specimens. The 35 species are drawn from 21 families, with their native ranges covering much of the world – particularly when considering the taxa at genus level (Fig. 3). The currently included taxa do, however, represent Europe more effectively than other areas, with none of the included species native to Australasia, New Zealand or much of Africa. This is a reflection of the author's location (the UK), which helped dictate both the accessibility of pollen material and priorities for engaging local audiences. Other areas were covered through a mixture of opportunistic and targeted sampling, some of it specifically aimed at specific regions or floras.

The 35 taxa included in the project to date cover a significant range of gross morphological characters (Fig. 2): monad (most taxa), pseudomonad (*Carex*), tetrad (*Drimys, Calluna*), and polyad (*Anadenanthera*); from oblate (*Tilia*) to prolate (*Centaurea, Quercus, Handroanthus*); colpate (*Salvia, Quercus*), porate (*Betula, Hordeum*), colporate (*Leucanthemum, Hedera*), poroid (*Carex*), heteroaperturate/pseudocolpate (*Miconia*), and sulcate (*Oenocarpus*); saccate (*Cedrus, Pinus*) and pear-shaped (*Carex*); echinate (*Leucanthemum, Ambrosia*), microechinate (*Artemisia*), echinolophate (*Scorzoneroides*), reticulate (*Drimys, Hedera, Salix*), striate (*Acer, Spondias*), scabrate (*Quercus, Filipendula*), areolate (*Dactylis*), and psilate (*Corylus, Betula*). Several taxa have multiple 3D model files which can be used to demonstrate the consequences of harmomegathy: the three Poaceae species show different ways in which their pollen grains can be deformed, for example, and *Quercus robur* and *Salvia pratensis* have pairs of models reflecting hydrated and dehydrated states with their attendant changes in shape (oblate/prolate) and polar view (circular/lobate). The models can even be used to demonstrate exines' relative flexibility, with some that show grains that were squashed between coverslip and slide (most notably *Echinacea angustifolia*).

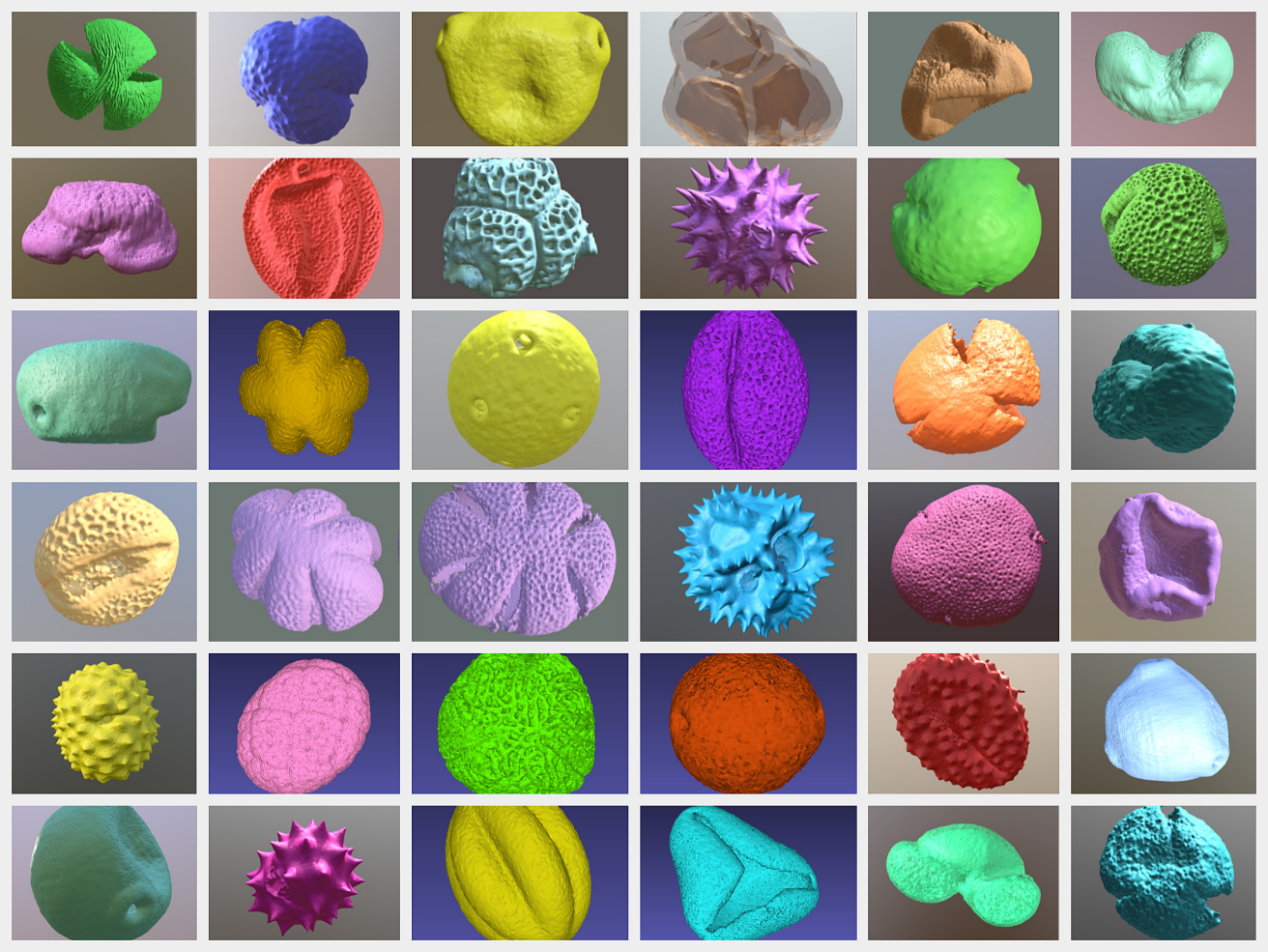

Fig. 2. Images of 36 of the 39 surface files currently available through the 3D Pollen Project, illustrating the range of morphological types that are included.

3. Results

3.1. Scan and model quality

Morphological features of the scanned pollen grains are generally faithfully captured by the scanning process described in Section 2.2. As noted in Section 2.1, CLSM resolution is always poorer in the z dimension (depth) than in x and y (eq. 1), and this can be seen in both scans and 3D models (Fig. 4) – it results, for example, in echini appearing broader from one side than another, and in surface ornamentation or apertures being less distinct on models' sides. Comparing the physical models with the scans also highlights that some fine features which are visible with the microscope (such as the tips of echini) become blunted in the surface models – in part this is due to limitations in CLSM resolution (Holt and Savoian, 2017), but it also comes about because signal intensity is lower in these features than elsewhere, so they are excluded by the threshold value used to reconstruct the grain's surface. Although these imperfections can be noticeable, and may need to be considered if using the scans or surface models as data, they are generally not problematic for most use cases. It was also possible to mitigate the loss of axial resolution in some models by reducing the CLSM pinhole size from 1 AU to 0.66 AU.

A critical consideration for the effective scanning of pollen grains is matching the refractive indices (RIs) of the sample mounting medium and the objective lens's immersion medium. The effect of RI matching/mismatching can be seen in Fig. 5. The RI-mismatched scan on the left side produced relatively lower signal which dropped off more markedly with depth than in the RI-matched sample on the right (a); compensating for this resulted in saturated scans at the grain's upper surface (b) while the lower levels still had low signal strength (a); and significant spherical aberration (the 'trail' at c) was present, resulting in the surface model having overly smoothed sides which are elongated below to produce a 'collar' effect at the bottom. By contrast, the RI-matched sample at right exhibited much less spherical aberration (c), retained more consistent signal strength with depth (a), and required less intense scanning: whereas the RI-mismatched image on the left of Fig. 5 is the sum of four individual scans, the RI-matched image on the right is a four-scan mean. The RI-mismatched sample's steep gradient of signal strength (a) could be somewhat reduced, and the saturated signal in its upper layers (b) eliminated, by modulating laser power while scanning the pollen grain (lowering the intensity for upper layers but increasing it with depth), but this approach would not address the weaker overall signal strength (a) or increased spherical aberration (c) that resulted from the RI mismatch, and so would have only limited utility.

3.2. The models in use

To the end of October 2022, the 3D Pollen Project's scan images and surface files have been downloaded over 6600 times and used in a wide range of activities around the world. The models are beginning to be used in pollen-related research (e.g. Park et al., 2021), but thus far the models' uses have predominantly been in public engagement and/or education. Unfortunately, the high-level data submitted at the point of

model download precludes a more granular overview of type, number and specific contexts of their uses.

Physical 3D pollen models have been incorporated into several natural history museum exhibitions, including at the Naturalis Biodiversity Center (the Netherlands), Georgia Museum of Natural History (USA), LWL-Museum für Naturkunde (Germany), and Steinhardt Museum of Natural History (Israel). Here, their value arises from being physical, visible representations of microscopic objects which cannot ordinarily be observed directly, and which have previously mostly been displayed as 2D images. The models' tactile nature has contributed to their successful use in many hands-on outreach sessions with diverse public audiences, such as 'science in the pub' talks, natural history museum school engagement activities, and stands at large public festivals. Being able to handle the models frequently prompts participants to ask questions about pollen – about the relationship between grains' appearance and allergenicity, the reasons for their varied shapes and forms, the purposes of apertures, etc. In some cases the models help people explore their existing relationships with pollen (through hay fever, very commonly), but often the questions appear to be prompted almost entirely by the experience of observing and handling the physical models. These provide many useful avenues for knowledge exchange about a range of different research areas. The striking and varied shapes of the pollen models have also led to their use at the interfaces of science and art, such as interactive sessions exploring pollen's role as a natural archive, or visual installations during public-facing science events, and their tactile nature has been leveraged in specially designed resources for visually impaired audiences.

The models have seen extensive use in educational settings. These uses have ranged from workshops on pollination with primary −/elementary-school children and elective classes on bio-inspired design in secondary/high schools, to university practical sessions on aerobiology and palaeoecology. In the latter case, the three-dimensional nature of the models can be especially useful for helping students to relate two-dimensional views of pollen grains from microscope observations to the structures of whole grains, such as assisting with determining the orientation of the grains and how changing focal depth helps to provide an overview of the sample. The biological accuracy of the models can also help students learn the different features of pollen grains – how various types of apertures, ornamentations and shapes appear, for example – as well as providing ways of illustrating how pollen grains can appear differently to those in identification keys (through dehydration, damage etc.). Additionally, the confocal microscope scans allow pollen grains' internal features to be easily highlighted (in greater resolution than through light microscopy, and in ways that scanning electron microscopy generally cannot), including in cross-sections of models or ones printed in translucent material. In this way, 3D pollen models could provide an innovation in the teaching of pollen identification; evaluation of their impact on teaching and learning is ongoing.

4. Discussion

So far, the 3D Pollen Project has provided a valuable resource to a wide range of communities for a diverse array of activities. The project's next steps aim to build on its existing successes, improve its relevance, and further broaden its utility by growing its coverage, enhancing the quality of its data, and developing the ways in which its resources are used.

An important next step in enhancing the value of the 3D Pollen Project is expanding its coverage of pollen morphology, phylogeny, and geographic and ecological gradients. For example, although all of the taxa sampled to date are seed plants, there is no reason in principle why pteridophytes and other spore-bearing plants could not be included. As Fig. 3 demonstrates, large parts of the world have few native pollen types included in the project, and the same will also be true of many ecosystems within apparently well-covered regions. This limits the applicability of the available resources for researchers, students and public audiences in many parts of the world. To remedy this, work is underway to identify and scan key pollen types for the world's ecoregions by integrating expert knowledge, floristic databases, and repositories of pollen data such as the Neotoma Palaeoecology Database (Dinerstein et al., 2017; Olson et al., 2001; Williams et al., 2018; https://neotomadb.org/). Additionally, while the dataset's current coverage of pollen's morphological traits is good, much of the structural diversity of the world's pollen – in which these traits appear in potentially millions of diverse combinations (Halbritter et al., 2018; Mander, 2016; Punt et al., 2007) – has yet to be included. Improving morphological coverage could go hand-in-hand with improving the dataset's phylogenetic coverage – using existing projects like the Evolution of Angiosperm Pollen series (Wortley et al., 2015) and phylomorphospatial methods (Jardine et al., 2022; Mander, 2016) to inform database expansions could allow the 3D pollen resources to support a wider array of scientific themes.

These steps will build the 3D Pollen Project into a geographically, ecologically, morphologically and phylogenetically representative sample of the world's pollen.

In order to facilitate a significant expansion of the 3D Pollen Project dataset, faster sample preparation is needed. As illustrated in Fig. 5, matching the refractive indices of the sample mountant and objective immersion medium is extremely important for good image quality, but mounting pollen grains in TDE is a time-consuming process: Staudt et al. (2007) recommend increasing the concentration of TDE in six steps, each of which takes 10 min or more, in addition to any other preparation steps such as acetolysis or removing samples from other mountants. It would be far more efficient to scan pre-existing pollen reference material, though this is typically mounted in silicone oil or glycerine jelly and so is RI-mismatched with standard immersion oil. A viable solution would be to use objective lenses specifically designed to work with silicone- or glycerine-mounted samples. Although less common than oil-immersion objectives, and with slightly lower numerical apertures (ca. 1.3 vs 1.4 for 63× objectives, which imposes a slight cost on image resolution – see eq. 1), these lenses could take high-quality, RI-matched scans directly from the many thousands of existing pollen reference slides held by research institutions. This step change in scanning efficiency could render feasible the wholesale, combined two- and three-dimensional digitisation of modern pollen reference collections (cf. Martin and Harvey, 2017).

There are several ways to improve the quality of the data captured in expanded 3D digitisation campaigns. It is possible, for example, for CLSMs to produce simultaneous transmitted light and confocal laser scans of the same pollen grains (Collings, 2015). Thus, individual samples could be viewed as with a light microscope, as higher-resolution cross-sections, and as a surface model; data from these three complementary modalities could provide significant benefits for individuals learning, demonstrating or investigating pollen morphology. Another possibility would be to use super-resolution confocal imaging techniques, which can provide comparable levels of detail to electron micrographs with less bespoke sample preparation, while also encoding 3D data (Romero et al., 2020b; Sivaguru et al., 2018). Romero et al. (2020b) note that silicone oil and glycerine are not ideal mountants for super-resolution confocal microscopy since they allow pollen grains to move, risking distortions in long scans, though both are considerably more viscous than TDE, which still produces detailed scans (Holt and Savoian, 2017; Vitha et al., 2010); more investigation into this question would be beneficial. If it could be done effectively, then using immersion-corrected objectives on a super-resolution CLSM to scan standard reference slides would represent a step change in the quantity and quality of 3D pollen data available to researchers and other audiences.

A much-enhanced dataset of 3D pollen scans and models could be used in a wide variety of ways. It could simply be used to expand the scope of the kinds of activities that have already taken place and/or to tailor them more precisely to local audiences/environments or specific

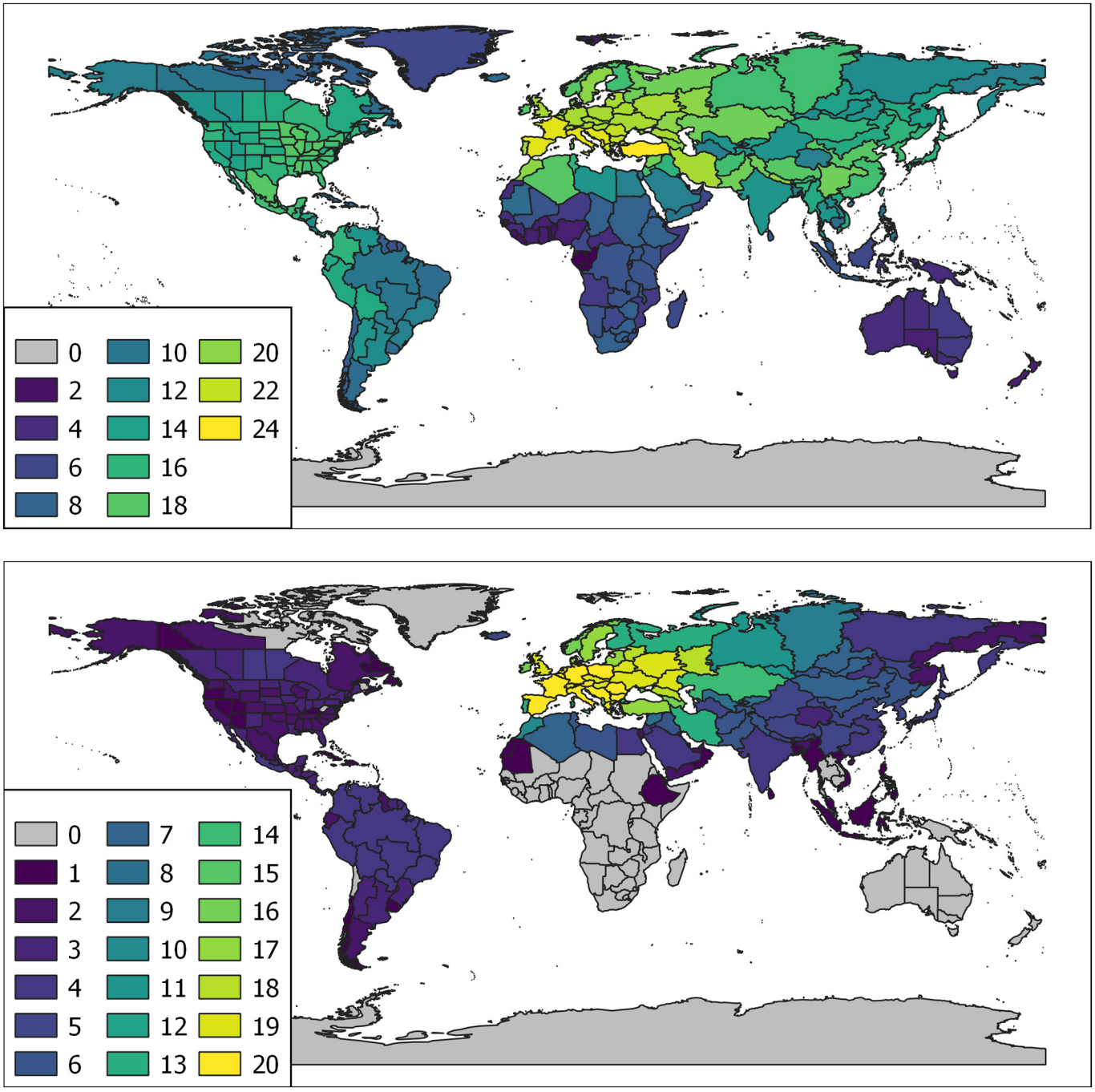

Fig. 3. Maps showing the number of taxa in the 3D Pollen Project (Table 1) with native distributions in different parts of the world at genus (top) and species (bottom) level. Only taxa identified to species are included. Data on native distributions (at level 3 in the TDWG geographical system) were taken from Plants of the World Online (POWO, 2022).

research contexts. However, its data could also be used to pioneer new and different kinds of knowledge exchange. Anecdotal evidence indicates that physical pollen models are appreciated by university students and teachers (a subject of ongoing pedagogical research), but it would also be possible to use the digital resources in teaching and learning. The importance of computer-based resources for teaching in palaeosciences gained significant recognition during the height of the Covid-19 pandemic (e.g. through the Virtual Palaeosciences project; Hutchinson et al., 2022), and pollen surface reconstructions could be used alongside transmitted light and confocal laser cross-section images to create digital slides for students to learn and practise pollen identification. If such resources (as complements to physical pollen models and other existing tools) make training in pollen identification significantly more accessible and engaging, it might even become feasible for citizen scientist 'para-palaeoecologists' to take part in this critical but exceptionally time-consuming part of palaeoecological research. (Notably, an alternative approach to streamlining this facet of palynology is automation, in which 3D pollen data can have a valuable role in algorithm training (Holt et al., 2011; Holt and Bebbington, 2014; Olsson et al., 2021; Romero et al., 2020a).) Such knowledge exchange need not be one-way, however. With an expanded dataset providing resources relevant to a wider range of people and ecosystems, which can lower the bar to engaging with and understanding palaeoecological research, it may become possible to use 3D pollen models to help bridge gaps

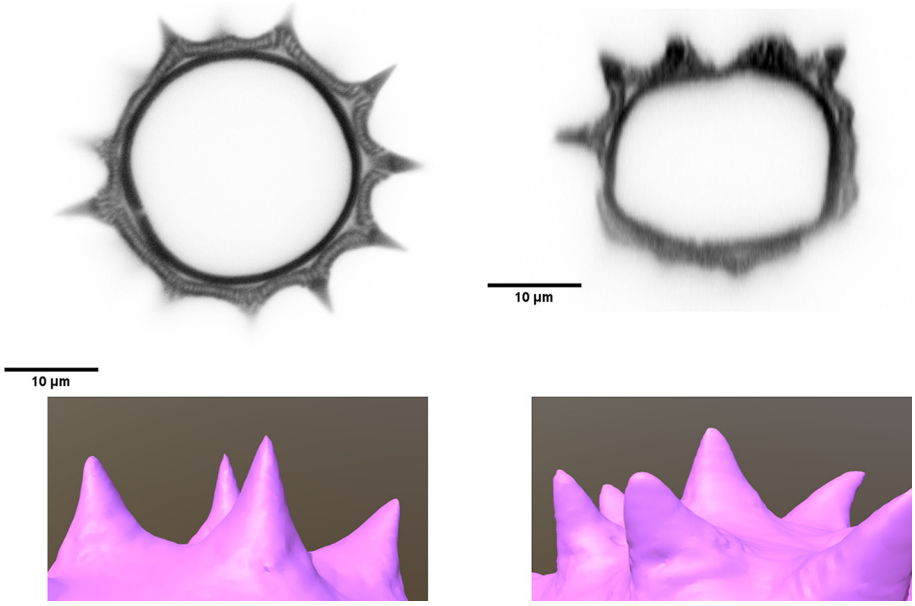

Fig. 4. Images showing the differences in scan resolution in xy/lateral (i.e. looking along the CLSM objective's line of sight; left) and xz/axial (i.e. looking 'side-on'; right) views in CLSM scans (top) and surface renderings (bottom) of *Echinacea angustifolia*. The CLSM images are single slices – unprocessed for the xy/lateral view (top left), and resliced and interpolated for the xz/axial view (top right).

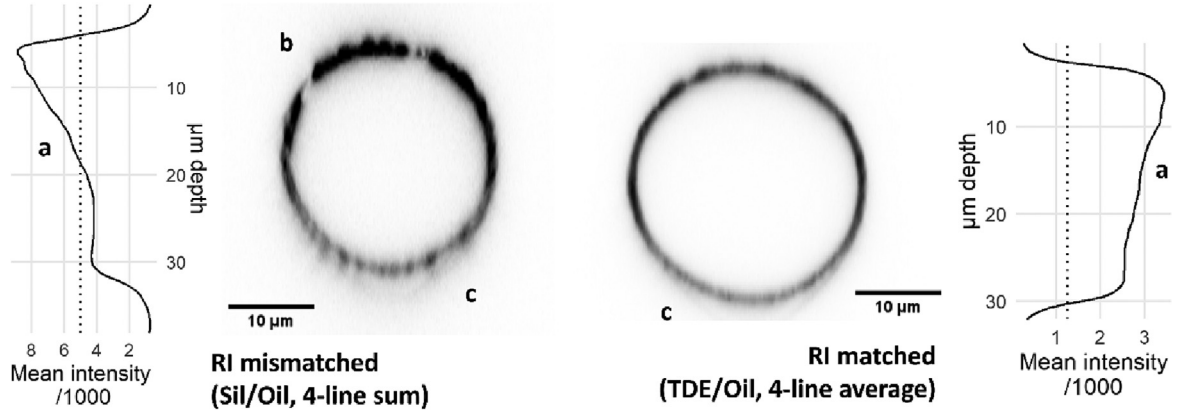

Fig. 5. Images showing key differences between RI-mismatched (silicone oil and immersion oil; left) and -matched (ca. 97% TDE and immersion oil; right) scans. The two central images show xz/axial cross-sections through Plantago pollen grains, and the graphs on the figure's edges show how signal intensity varies with depth through the cross-sections. The RI-mismatched image on the left is the sum of four scans; the RI-matched image on the left is the mean of four scans. The dotted vertical lines in the graphs allow a comparison of relative signal intensities: the line for the RI-mismatched image at left is at an intensity of 5000 – four times its value of 1250 in the RI-matched image at right. Letter annotations identify features discussed in the main text: a – differences in signal loss with depth; b – saturation in upper slices of the mismatched scan; c – differences in spherical aberration.

between researchers and holders of local/traditional ecological knowledge. Ultimately, bringing together these different ways of understanding could provide novel and holistic insights into past (socio-)ecological systems (Lynch et al., 2020; Lyver et al., 2015; Richer and Gearey, 2017; Zurita-Benavides et al., 2016).

5. Conclusions

Biologically accurate, larger-than-life 3D-printed models of pollen grains are effective tools for engaging non-expert audiences with pollen and related research, which can otherwise appear hard to grasp. The 3D Pollen Project has to date used confocal laser scanning microscopy to produce high-resolution scans and surface models of 35 taxa, making the outputs freely available online. Assisted by effective sample preparation and imaging protocols, the sampled taxa encompass a broad and widely applicable range of morphological features, allowing resources to be used more broadly than their species' native distributions might suggest. Scans and digital and physical models have been used in varied and creative ways across a wide spectrum of contexts, from natural history museums to classrooms and art exhibitions to scientific research. The range of the resources' applications has been facilitated to a great extent by making them available online with no cost and minimal licencing restrictions. Future work – expanding the project's coverage to include more of the world's ecosystems and pollen types, further improving the quality of the data generated, and continuing to investigate the resources' potential applications – will help the 3D Pollen Project to engage an increasingly diverse range of audiences with the fascinating world of pollen and the sciences which study it.

Data availability

Data from the 3D Pollen Project are available under a CC-BY-NC (Creative Commons, attribution, non-commercial) licence from the MorphoSource repository: https://www.morphosource.org/Detail/

ProjectDetail/Show/project_id/627. Further details can be found on the 3D Pollen Project website: https://3dpollenproject.wixsite.com/main/.

Declaration of Competing Interest

The author declares that he has no known competing financial interests or personal relationships that could have appeared to influence the work reported in this paper.

Acknowledgements

Many people have helped and supported the 3D Pollen Project along its journey. The work described took place alongside my PhD at the University of Reading, which was supervised by Francis Mayle and funded by a University of Reading Graduate Teaching Assistant studentship, and when I was a visiting student at the University of Hull with M. Jane Bunting. I am grateful to Cordula Kemp and Ann Lowry at Hull for their assistance with the confocal microscopy. My thanks go to everyone who has provided support and encouragement at various stages of the project, particularly Katherine Holt, Hannah Worthen, Francis Mayle, M. Jane Bunting and Robert Marchant. M. Jane Bunting (HLU-CCC samples), Alastair Culham (RNG-P…), Francis Mayle (RNG-TPRG), Felipe Franco-Gaviria (EXR-EXPR), Benjamin Bell (MANCH-PolRefCol) and Stuart Wagenius, Gabriel Hutchinson and Michael LaScaleia (CHIC-EchProj) provided the samples incorporated in the project so far; thank you too to everyone who has sent specimens which have still to be included in the database. Work on the 3D Pollen Project continues under a postdoctoral Knowledge Exchange Fellowship at the University of York, funded by the UK's Natural Environment Research Council. I thank Robert Marchant and Francis Mayle for their helpful comments on an earlier draft of this manuscript, as well as two anonymous reviewers for their constructive feedback.

The 3D Pollen Project has been funded by Mangorolla CIC through the 'I'm A Scientist' competition (Neptunium Zone, 2017), the University of Reading Teaching and Learning Development Fund (TLDF_mini/2018/126, A3591410), and the Natural Environment Research Council (NE/X001660/1).

References

Arganda-Carreras, I., Kaynig, V., Rueden, C., Eliceiri, K.W., Schindelin, J., Cardona, A., Seung, H.S., 2017. Trainable Weka Segmentation: a machine learning tool for microscopy pixel classification. Bioinformatics 33, 2424–2426. https://doi.org/10.1093/bioinformatics/btx180.

Atwe, S.U., Ma, Y., Gill, H.S., 2014. Pollen grains for oral vaccination. J. Control. Release 194, 45–52. https://doi.org/10.1016/j.jconrel.2014.08.010.

Ball, A.D., Job, P.A., Walker, A.E.L., 2017. SEM-microphotogrammetry, a new take on an old method for generating high-resolution 3D models from SEM images. J. Microsc. 267, 214–226. https://doi.org/10.1111/jmi.12560.

Banks, H., Rudall, P.J., 2016. Pollen structure and function in caesalpinioid legumes. Am. J. Bot. 103, 423–436. https://doi.org/10.3732/ajb.1500248.

Carvalho, M.R., Jaramillo, C., de la Parra, F., Caballero-Rodríguez, D., Herrera, F., Wing, S., Turner, B.L., D'Apolito, C., Romero-Báez, M., Narváez, P., Martínez, C., Gutierrez, M., Labandeira, C., Bayona, G., Rueda, M., Paez-Reyes, M., Cárdenas, D., Duque, Á., Crowley, J.L., Santos, C., Silvestro, D., D'Apolito, C., Romero-Báez, M., Narváez, P., Martínez, C., Gutierrez, M., Labandeira, C., Bayona, G., Rueda, M., Paez-Reyes, M., Cárdenas, D., Duque, Á., Crowley, J.L., Santos, C., Silvestro, D., 2021. Extinction at the end-Cretaceous and the origin of modern Neotropical rainforests. Science (80-.) 372, 63–68. https://doi.org/10.1126/science.abf1969.

Cignoni, P., Callieri, M., Corsini, M., Dellepiane, M., Ganovelli, F., Ranzuglia, G., 2008. MeshLab: an open-source mesh processing tool. 6th Eurographics Italian Chapter Conference 2008 - Proceedings, pp. 129–136.

Collings, D.A., 2015. Optimisation approaches for concurrent transmitted light imaging during confocal microscopy. Plant Methods 11, 40. https://doi.org/10.1186/s13007-015-0085-3.

D'Amato, G., Cecchi, L., Bonini, S., Nunes, C., Annesi-Maesano, I., Behrendt, H., Liccardi, G., Popov, T., van Cauwenberge, P., 2007. Allergenic pollen and pollen allergy in Europe. Allergy 62, 976–990. https://doi.org/10.1111/j.1398-9995.2007.01393.x.

Diel, E.E., Lichtman, J.W., Richardson, D.S., 2020. Tutorial: avoiding and correcting sample-induced spherical aberration artifacts in 3D fluorescence microscopy. Nat. Protoc. 15, 2773–2784. https://doi.org/10.1038/s41596-020-0360-2.

Dinerstein, E., Olson, D., Joshi, A., Vynne, C., Burgess, N.D., Wikramanayake, E., Hahn, N., Palminteri, S., Hedao, P., Noss, R., Hansen, M., Locke, H., Ellis, E.C., Jones, B., Barber, C.V., Hayes, R., Kormos, C., Martin, V., Crist, E., Sechrest, W., Price, L., Baillie, J.E.M., Weeden, D., Suckling, K., Davis, C., Sizer, N., Moore, R., Thau, D., Birch, T., Potapov, P., Turubanova, S., Tyukavina, A., de Souza, N., Pintea, L., Brito, J.C., Llewellyn, O.A., Miller, A.G., Patzelt, A., Ghazanfar, S.A., Timberlake, J., Klöser, H., Shennan-Farpón, Y., Kindt, R., Lillesø, J.-P.B., van Breugel, P., Graudal, L., Voge, M., Al-Shammari, K.F., Saleem, M., 2017. An ecoregion-based approach to protecting half the terrestrial realm. Bioscience 67, 534–545. https://doi.org/10.1093/biosci/bix014.

Faegri, K., Iversen, J., 1964. Textbook of Pollen Analysis. Second edi. ed. John Wiley & Sons Ltd, Chichester, UK.

French, C., Hunt, C.O., Grima, R., McLaughlin, R., Stoddart, S., Malone, C. (Eds.), 2020. Temple Landscapes: Fragility, Change and Resilience of Holocene Environments in the Maltese Islands. McDonald Institute for Archaeological Research, Cambridge, UK.

Guzmán-Delgado, P., Zwieniecki, M.A., 2019. The makeup of a gamete space capsule. Nat. Plants 5, 8. https://doi.org/10.1038/s41477-018-0342-3.

Halbritter, H., Ulrich, S., Grímsson, F., Weber, M., Zetter, R., Hesse, M., Buchner, R., Svojtka, M., Frosch-Radivo, A., 2018. Illustrated Pollen Terminology. Springer International Publishing, Cham https://doi.org/10.1007/978-3-319-71365-6.

Harris, T.L., Wenthur, C.J., Diego-Taboada, A., Mackenzie, G., Corbitt, T.S., Janda, K.D., 2016. Lycopodium clavatum exine microcapsules enable safe oral delivery of 3,4-diaminopyridine for treatment of botulinum neurotoxin a intoxication. Chem. Commun. 52, 4187–4190. https://doi.org/10.1039/c6cc00615a.

Holt, K., Bebbington, M.S., 2014. Separating morphologically similar pollen types using basic shape features from digital images: a preliminary study. Appl. Plant Sci. 2, 1400032. https://doi.org/10.3732/apps.1400032.

Holt, K.A., Savoian, M.S., 2017. Epi-fluorescence microscopy and 3D printing: An easily implemented approach for producing accurate physical models of micro- and macro-scopic biological samples. In: Méndez-Vilas, A. (Ed.), Microscopy and Imaging Science: Practical Approaches to Applied Research and Education. Formatex Research Centre, Badajoz, Spain, pp. 697–702.

Holt, K., Allen, G., Hodgson, R., Marsland, S., Flenley, J., 2011. Progress towards an automated trainable pollen location and classifier system for use in the palynology laboratory. Rev. Palaeobot. Palynol. 167, 175–183. https://doi.org/10.1016/j.revpalbo.2011.08.006.

Hutchinson, S.M., Bacon, K.L., Bunting, M.J., Hurrell, E.R., 2022. The Virtual Palaeosciences (ViPs) project: resources for online learning in or out of a pandemic. J. Geogr. High. Educ. 1–11. https://doi.org/10.1080/03098265.2022.2129599.

Jardine, P.E., Palazzesi, L., Tellería, M.C., Barreda, V.D., 2022. Why does pollen morphology vary? Evolutionary dynamics and morphospace occupation in the largest angiosperm order (Asterales). New Phytol. 234, 1075–1087. https://doi.org/10.1111/NPH.18024.

Jarzen, D.M., Jarzen, S.A., 2006. Collecting pollen and spore samples from herbaria. Palynology 30, 111–119. https://doi.org/10.2113/gspalynol.30.1.111.

Kelly, T.J., Lawson, I.T., Roucoux, K.H., Baker, T.R., Honorio-Coronado, E.N., Jones, T.D., Rivas Panduro, S., 2018. Continuous human presence without extensive reductions in forest cover over the past 2500 years in an aseasonal Amazonian rainforest. J. Quat. Sci. 33, 369–379. https://doi.org/10.1002/jqs.3019.

Kesseler, R., Harley, M.M., 2009. Pollen: The Hidden Sexuality of Flowers. Papdakis Publishers, London.

Li, F.-S., Phyo, P., Jacobowitz, J., Hong, M., Weng, J.-K., 2019. The molecular structure of plant sporopollenin. Nat. Plants 5, 41–46. https://doi.org/10.1038/s41477-018-0330-7.

Lynch, A.J.J., Ferrier, Ford, A.J., Haberle, S.G., Rule, S., Schneider, L., Zawadzki, A., Metcalfe, D.J., 2020. Rainforest, woodland or swampland? Integrating time, space and culture to manage an endangered ecosystem complex in the Australian Wet Tropics. Landsc. Ecol. 35, 83–99. https://doi.org/10.1007/s10980-019-00931-7.

Lyver, P.O.B., Wilmshurst, J.M., Wood, J.R., Jones, C.J., Fromont, M., Bellingham, P.J., Stone, C., Sheehan, M., Moller, H., 2015. Looking back for the future: local knowledge and palaeoecology inform biocultural restoration of coastal ecosystems in New Zealand. Hum. Ecol. 43, 681–695. https://doi.org/10.1007/s10745-015-9784-7.

Mackenzie, G., Boa, A.N., Diego-Taboada, A., Atkin, S.L., Sathyapalan, T., 2015. Sporopollenin, the least known yet toughest natural biopolymer. Front. Mater. 2, 66. https://doi.org/10.3389/fmats.2015.00066.

Maezumi, S.Y., Alves, D., Robinson, M., de Souza, J.G., Levis, C., Barnett, R.L., Almeida de Oliveira, E., Urrego, D., Schaan, D., Iriarte, J., 2018. The legacy of 4,500 years of polyculture agroforestry in the eastern Amazon. Nat. Plants 4, 540–547. https://doi.org/10.1038/s41477-018-0205-y.

Mander, L., 2016. A combinatorial approach to angiosperm pollen morphology. Proc. R. Soc. B Biol. Sci. 283. https://doi.org/10.1098/rspb.2016.2033.

Martin, A.C., Harvey, W.J., 2017. The Global Pollen Project: a new tool for pollen identification and the dissemination of physical reference collections. Methods Ecol. Evol. 8, 892–897. https://doi.org/10.1111/2041-210X.12752.

Mildenhall, D., 2008. Civil and criminal investigations. The use of spores and pollen. SIAK-J. — Zeitschrift für Polizeiwiss. und polizeiliche Prax, 35–52 https://doi.org/10.7396/2008_4_E.

Morris, J.L., Puttick, M.N., Clark, J.W., Edwards, D., Kenrick, P., Pressel, S., Wellman, C.H., Yang, Z., Schneider, H., Donoghue, P.C.J., 2018. The timescale of early land plant evolution. Proc. Natl. Acad. Sci. U. S. A. 115, E2274–E2283. https://doi.org/10.1073/pnas.1719588115.

Mottl, O., Flantua, S.G.A., Bhatta, K.P., Felde, V.A., Giesecke, T., Goring, S., Grimm, E.C., Haberle, S., Hooghiemstra, H., Ivory, S., Kuneš, P., Wolters, S., Seddon, A.W.R., Williams, J.W., 2021. Global acceleration in rates of vegetation change over the past 18,000 years. Science (80-.) 372, 860–864. https://doi.org/10.1126/science.abg1685.

Olson, D.M., Dinerstein, E., Wikramanayake, E.D., Burgess, N.D., Powell, G.V.N., Underwood, E.C., D'Amico, J.A., Itoua, I., Strand, H.E., Morrison, J.C., Loucks, C.J., Allnutt, T.F., Ricketts, T.H., Kura, Y., Lamoreux, J.F., Wettengel, W.W., Hedao, P., Kassem, K.R., 2001. Terrestrial ecoregions of the world: a new map of life on Earth. Bioscience 51, 933–938. https://doi.org/10.1641/0006-3568(2001)051[0933:TEOTWA]2.0.CO;2.

Olsson, O., Karlsson, M., Persson, A.S., Smith, H.G., Varadarajan, V., Yourstone, J., Stjernman, M., 2021. Efficient, automated and robust pollen analysis using deep learning. Methods Ecol. Evol. 12, 850–862. https://doi.org/10.1111/2041-210X.13575.

Park, S., Finkelman, L., Yossifon, G., 2021. Enhanced cargo loading of electrically powered metallo-dielectric pollen bearing multiple dielectrophoretic traps. J. Colloid Interface Sci. 588, 611–618. https://doi.org/10.1016/j.jcis.2020.10.147.

Pawankar, R., Canonica, G., Holgate, S., Lockey, R., 2013. World Allergy Organization (WAO) White Book on Allergy: Update 2013. World Allergy Organization.

Perry, I., Szeto, J.-Y., Isaacs, M., Gealy, E., Rose, R., Scofield, S., Watson, P., Hayes, A., 2017. Production of 3D printed scale models from microscope volume datasets for use in STEM education. EMS Eng. Sci. J. 1, 002.

Porto, R.G., de Almeida, R.F., Cruz-Neto, O., Tabarelli, M., Viana, B.F., Peres, C.A., Lopes, A.V., 2020. Pollination ecosystem services: a comprehensive review of economic values, research funding and policy actions. Food Secur. 12, 1425–1442. https://doi.org/10.1007/s12571-020-01043-w.

POWO, 2022. Plants of the World Online. Facilitated by the Royal Botanic Gardens, Kew [WWW Document]. http://www.plantsoftheworldonline.org/ accessed 11.7.22.

Punt, W., Hoen, P.P., Blackmore, S., Nilsson, S., Le Thomas, A., 2007. Glossary of pollen and spore terminology. Rev. Palaeobot. Palynol. 143, 1–81. https://doi.org/10.1016/j.revpalbo.2006.06.008.

Richer, S., Gearey, B., 2017. The medicine tree: unsettling palaeoecological perceptions of past environments and human activity. J. Soc. Archaeol. 17, 239–262. https://doi.org/10.1177/1469605317731013.

Roberts, N., 2014. The Holocene: An Environmental History. Third Edit. ed. John Wiley & Sons, Incorporated, Chichester, UK.

Rodrguez-Forero, G., Oboh-Ikuenobe, F.E., Jaramillo-Munoz, C., Rueda-Serrano, M.J., Cadena-Rueda, E., 2012. Palynology of the Eocene Esmeraldas formation, Middle Magdalena Valley Basin, Colombia. Palynology 36, 96–111. https://doi.org/10.1080/01916122.2012.650548.

Romero, I.C., Kong, S., Fowlkes, C.C., Jaramillo, C., Urban, M.A., Oboh-Ikuenobe, F., D'Apolito, C., Punyasena, S.W., 2020a. Improving the taxonomy of fossil pollen using convolutional neural networks and superresolution microscopy. Proc. Natl. Acad. Sci. 117, 28496–28505. https://doi.org/10.1073/pnas.2007324117.

Romero, I.C., Urban, M.A., Punyasena, S.W., 2020b. Airyscan superresolution microscopy: a high-throughput alternative to electron microscopy for the visualization and analysis of fossil pollen. Rev. Palaeobot. Palynol. 276, 104192. https://doi.org/10.1016/j.revpalbo.2020.104192.

Rubinstein, C.V., Gerrienne, P., de la Puente, G.S., Astini, R.A., Steemans, P., 2010. Early Middle Ordovician evidence for land plants in Argentina (eastern Gondwana). New Phytol. 188, 365–369. https://doi.org/10.1111/j.1469-8137.2010.03433.x.

Rull, V., Cañellas-Boltà, N., Margalef, O., Pla-Rabes, S., Sáez, A., Giralt, S., 2016. Three millennia of climatic, ecological, and cultural change on Easter Island: an integrative overview. Front. Ecol. Evol. 4, 1–4. https://doi.org/10.3389/fevo.2016.00029.

Schindelin, J., Arganda-Carreras, I., Frise, E., Kaynig, V., Longair, M., Pietzsch, T., Preibisch, S., Rueden, C., Saalfeld, S., Schmid, B., Tinevez, J.Y., White, D.J., Hartenstein, V., Eliceiri, K., Tomancak, P., Cardona, A., 2012. Fiji: an open-source platform for biological-image analysis. Nat. Methods https://doi.org/10.1038/nmeth.2019.

Schmid, B., Schindelin, J., Cardona, A., Longair, M., Heisenberg, M., 2010. A high-level 3D visualization API for Java and ImageJ. BMC Bioinformatics 11, 274. https://doi.org/10.1186/1471-2105-11-274.

Sivaguru, M., Urban, M.A., Fried, G., Wesseln, C.J., Mander, L., Punyasena, S.W., 2018. Comparative performance of airyscan and structured illumination superresolution microscopy in the study of the surface texture and 3D shape of pollen. Microsc. Res. Tech. 81, 101–114. https://doi.org/10.1002/jemt.22732.

Staudt, T., Lang, M.C., Medda, R., Engelhardt, J., Hell, S.W., 2007. 2,2′-Thiodiethanol: a new water soluble mounting medium for high resolution optical microscopy. Microsc. Res. Tech. 70, 1–9. https://doi.org/10.1002/jemt.20396.

Stevenson, J., Kaikkonen, T., 2019. Creating a hand-held microscopic world. Quat. Australas. 36, 22–25.

Uddin, M.J., Gill, H.S., 2018. From allergen to oral vaccine carrier: a new face of ragweed pollen. Int. J. Pharm. 545, 286–294. https://doi.org/10.1016/j.ijpharm.2018.05.003.

Vitha, S., Bryant, V.M., Zwa, A., Holzenburg, A., 2010. 3D confocal imaging of pollen. Micros. Today 18, 26–28. https://doi.org/10.1017/S1551929510000039.

Wallace, S., Fleming, A., Wellman, C.H., Beerling, D.J., 2011. Evolutionary development of the plant spore and pollen wall. AoB Plants 11. https://doi.org/10.1093/aobpla/plr027.

Weisshart, K., 2014. The Basic Principle of Airyscanning. Jena.

Wellman, C.H., 2010. The invasion of the land by plants: when and where? New Phytol. https://doi.org/10.1111/j.1469-8137.2010.03471.x.

Williams, J.W., Shuman, B.N., Webb, T., Bartlein, P.J., Leduc, P.L., 2004. Late-Quaternary vegetation dynamics in North America: scaling from taxa to biomes. Ecol. Monogr. 74, 309–334. https://doi.org/10.1890/02-4045.

Williams, John W., Grimm, Eric C., Blois, J.L., Charles, D.F., Davis, E.B., Goring, S.J., Graham, R.W., Smith, A.J., Anderson, M., Arroyo-Cabrales, J., Ashworth, A.C., Betancourt, J.L., Bills, B.W., Booth, R.K., Buckland, P.I., Curry, B.B., Giesecke, T., Jackson, S.T., Latorre, C., Nichols, J., Purdum, T., Roth, R.E., Stryker, M., Takahara, H., Williams, J.W., Grimm, E.C., 2018. The Neotoma Paleoecology Database, a Multiproxy, International, Community-Curated Data Resource. 89, pp. 156–177. https://doi.org/10.1017/qua.2017.105.

Wortley, A.H., Wang, H., Lu, L., Li, D., Blackmore, S., 2015. Evolution of Angiosperm Pollen. 1. Introduction. Ann. Missouri Bot. Gard. 100, 177–226. https://doi.org/10.3417/2012047.

Zurita-Benavides, M.G., Jarrín-V, P., Rios, M., 2016. Oral history reveals landscape ecology in ecuadorian Amazonia: time categories and ethnobotany among Waorani people. Econ. Bot. 70, 1–14. https://doi.org/10.1007/s12231-015-9330-y.